Visual Abstract

Effect of friction-welding parameters on the tensile strength of AA6063 with dissimilar joints

Yashwant U. Chapke, Dinesh N. Kamble
Department of Mechanical Engineering, Vishwakarma Institute of Information Technology, Savitribai Phule Pune University, India
yashchapke@gmail.com; http://orcid.org/ 0000-0002-6843-7415
dnkamble81@gmail.com; http://orcid.org/ 0000-0002-1312-2619

ABSTRACT. In this paper, the effect of welding parameters of rotary friction welding between AA6063 and AISI4130 and AA6063 and Copper are investigated. The major influencing parameters considered are upset pressure, friction time and friction pressure of friction welding are considered for this study. The Taguchi's design of experiments was conducted for the influencing parameters and their levels. The tensile test experimentation was carried out and the results of the AA6063 and AISI4130 and AA6063 and Copper are compared. The ultimate tensile strength of AA6063-AISI4130 joint and AA6063-Copper joint was improved by increasing upset pressure up to 97MPa with FP of 71 MPa and FT of 4 sec. On the side of AA6063, intermetallic compounds have formed, as seen in SEM micrographs. Microcracks are forming on the side of AA6063 and propagates along the grain boundaries. The effect of the influencing parameters on the tensile strength of the dissimilar joints are studied using the Taguchi's DOE and ANOVA. From the outcomes it is observed that the friction pressure influence more on the strength of the AA6063 dissimilar joints.

KEYWORDS. AA6063; Copper; AISI4130; Friction welding; Taguchi's DOE.

OPEN ACCESS

Citation: Chapke, Y. U, Kamble, D. N., Effect of friction-welding parameters on the tensile strength of AA6063 with dissimilar joints, Frattura ed Integrità Strutturale, 62 (2022) 573-584.

Received: 01.08.2022
Accepted: 12.09.2022
Online first: 13.09.2022
Published: 01.10.2022

INTRODUCTION

One of the most effective method to join the dissimilar metals is rotary friction welding (RFW) which is economic and provides safety to operator and does not emit the IR rays, fume and smoke during the welding [1-2]. The application of RFW, in many industries such as aircraft structures and aero engine components, is required to join dissimilar metals which is inevitable now a days [3-4]. Similar to it, linear friction welding (LFW) and inertia friction welding (IFW) were also used to join the dissimilar metals which gain the more interest now a days [5-6]. In welding of aluminium-stainless steel dissimilar metals using inertia friction welding, the intermetallic compound layer generated at the interface of joining which was seen to be increases with the increment in the rotational speed [7]. These innovative welding techniques to join the dissimilar metals plays the important role in the automobile industry where it requires light weight structures with high strength to weight ratio for automobiles. Thus, the friction welding method becomes the

highly efficient [8] and promising technology to weld the dissimilar metals with narrow heat-affected zone (HAZ) [9]. In friction welding, among the two dissimilar metal rods, one of them is held in the chuck and rotating and another rod is fixed in the pneumatic holder. Th axial load applied by the pneumatic holder generates the frictional heat which necessary to weld both rods together. The friction welding (FW) machine generates the required heat to weld the two dissimilar rods through their surface interaction while rotating. This welding is possible due to the intermolecular diffusion formed between the faces of two dissimilar rods. In the friction welding, the heat generated at the interface is lower than the melting temperature of base metals [10]. Thus, the melting of metals will not happen in it.

To get the strong joint, the factors like upset pressure (UP), friction time (FT) and friction pressure (FP) influence significantly [11]. However, when the friction and upset pressure increases the heat generated and extruded metal heat also increases. In case of FW of aluminum and steel, the probability of generation of thin intermetallic compounds, which were brittle in nature [12-13]. The intermetallics, such as FeAl and Fe_2Al_5, were formed in the process of FW of the AA6061-AISI1018 steel [3]. The increase in friction time during friction welding while joining of AA6063 with SS304 [14], at low pressure, leads to increment in the temperature which softens the weld. Thus, the increment in the temperature, due to higher pressure and FT, and cooling rate causes the inducement of residual stress in the welded joints.

The addition of the nickel interlayer enhances the tensile strength [15] and addition of silver causes the reduction of magnesium in aluminum and reduces the width of intermetallic layer and enhances the tensile strength [16]. While joining of AA5052 and AA6063 with the friction welding, Adrian Lis et al. [17] observed that lower friction pressure causes the reduction in the thickness of the soft HAZ in turn increases the tensile strength of the welded joint. Ajith et al. [18] studied the FW of the S32205 duplex stainless steel and concluded the upset and FP were the majorly influencing process parameters. Many authors [19-22] used Taguchi's method of optimization and design of experiments (DOE) [23] to study the effect of process parameters.

Literatures shows the dissimilar metals like aluminum-steel, steel-copper alloys, carbon-stainless steel, carbon steel-aluminium are welded using the friction welding [24-28]. The joint's tensile strength will be affected by changes in pressure and time because the base metals' have different coefficients of thermal expansion. The objective of present work is to find the influence of the process parameters on the tensile strength of AA6063-AISI4130 and AA6063-Cu dissimilar welding joints. In this work, it is intended to use RFW to combine AA6063 with AISI4130 steel and AA6063 with copper specimens. The main purpose of this work is to identify the RFW parameters to weld the dissimilar metals, like, steel and copper with aluminum to reduce the weight of the machine components. Some of the applications where RFW of aluminum with steel are Axle shafts, driveshafts, gears to shafts, hydraulic cylinder rod end, pipe to pipe segments etc. This study is for determining the influence of FW parameters utilized for welding of dissimilar metals on their tensile strength. The Taguchi's DOE and ANOVA has been utilized to analyze the experimental outcomes. The confirmation experiment will also be carried out to validate the experimental results.

MATERIALS AND PREPARATION

The materials chosen for this work are aluminum 6063 alloy, AISI4130 low alloy steel and copper in industrial and domestic applications. The chemical composition of AA6063, AISI4130 are listed in Tab. 1(a-b).

Element	Ti	Cu	Fe	Zn	Si	Mg	Mn	Cr	Al
Composition	0.02	0.029	0.26	0.061	0.50	0.4	0.045	0.01	98.57

Table 1(a): Chemical composition of AA6063 [29]

Element	C	Mn	Pmax	Smax	Si	Cr	Mo	Fe
Composition	0.03	0.60	0.008	0.010	0.23	0.80	0.25	Balance

Table 1(b): Chemical composition of the AISI4130 steel [30].

Property	Density	Tensile strength	Yield strength	Elastic modulus	Elongation
Composition	8.93g/cm^3	210MPa	33MPa	110GPa	60%

Table 1(c): Properties of the copper [31].

AISI4130 steels have enhanced properties like corrosion resistance, ductile, moderate hardness, higher strength and flexibility and able to withstand shock loads. It is having the low carbon content up to 0.03%. Its major alloying elements

are Cr, Mn and Mo. Aluminum 6063 alloy have silicon, iron and magnesium as major alloying elements. Copper is the soft, ductile and malleable metal and its melting point is 1084^{o}C. Among many excellent properties of copper, electrical conductivity, thermal conductivity are the properties which makes the copper to be used in electrical parts, due to the high corrosion resistance of copper, it can also be find applications in marine, gas and domestic plumbing industries. Some of the material properties of copper are listed in Tab. 1(c).

METHODS

Welding parameters selection

Detailed study on rotary friction welding shows the possibility of effect of its process parameters on the joint and its strength. Parameters influencing tensile strength of RFW joint are UP, FP, FT and spindle speed (SS). In this work, the keeping the spindle speed (SS) constant at 1500 rpm, the other parameters such as FP, FT and UP are varied which influences majorly on tensile strength of welded joint. With the increase of process parameters, to analyze the data, large number of samples must be experimented. Taguchi's design of experiment (DOE) will provide the special design of orthogonal arrays which gives the minimum sets of experiments to analyze the data effectively. Taguchi Method is a statistical method for improving quality & is based on three loss function viz., Larger is better, Smaller is better and Nominal is better and hitting the target with minimum variation.

The Taguchi's DOE is carried out using the commercially available statistical tool for the process parameters FP, FT and UP with the three levels as mentioned in the Tab. 2. The levels considered in this work are based on the literature referred and as per the specification of the RFW machine available. Tab. 3 list the design of experiments (DOE) carried out using the Taguchi's L9 orthogonal array.

Process Parameter	FP, MPa	FT, Sec	UP, MPa
Level 1	48	2	38
Level 2	71	4	68
Level 3	97	6	97

Table 2: Levels of process parameters considered.

Case	Friction Pressure MPa	Friction Time Sec	Upset Pressure MPa
1	48	2	38
2	48	4	68
3	48	6	97
4	71	2	68
5	71	4	97
6	71	6	38
7	97	2	97
8	97	4	38
9	97	6	68

Table 3: Experimental Trail Run using DOE.

Experimentation

Fig.1 shows the RFW machine, where workpiece 1 (AA6063) is fixed in chuck and rotating at 1500rpm and the workpiece 2 (AISI4130/Cu) is held in pneumatic holder which pushes it in axial direction for certain time (FP).

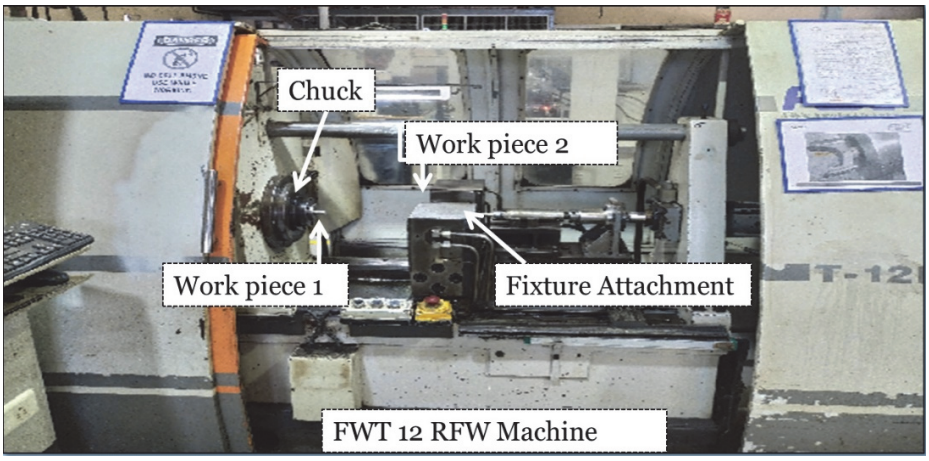

Figure 1: Experimental set up (Rotary Friction Welding Machine) FT 12.

The workpiece (AA6063, AISI4130 and Copper) dimensions considered are 25mm diameter and length 100mm. The surfaces of the workpieces are prepared well so that welding surface will be free from imperfections. In this welding, joining of dissimilar metals requires influence of pressure and relative motion of the two workpieces.
In comparison with steel and copper, degree of deformation is larger for aluminum. Thus, the weld flash on AA6063 is larger (shown in Fig.2). Due to higher thermal conductivity of AA6063, it is cooled fast then the steel. The Fig. 2 shows the welded samples of AA6063-AISI4130 and AA6063-Cu using the RFW.

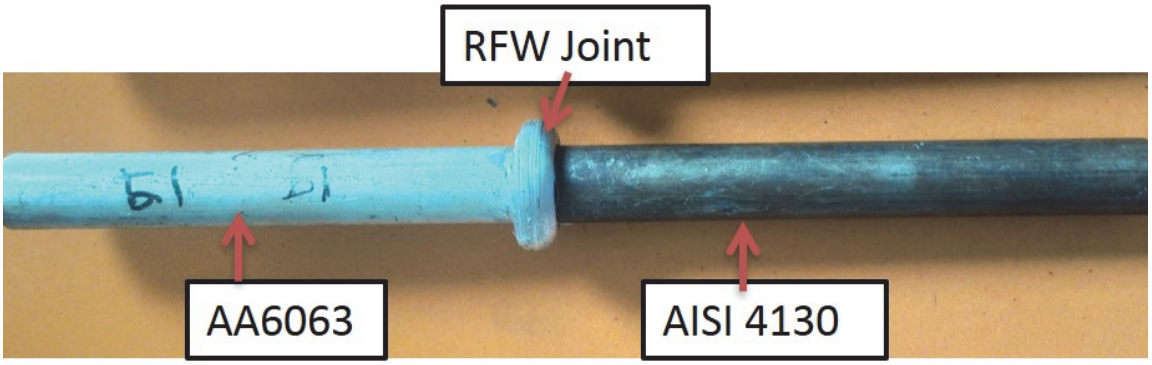

Figure 2(a): Specimens Prepared using AA6063 and AISI4130.

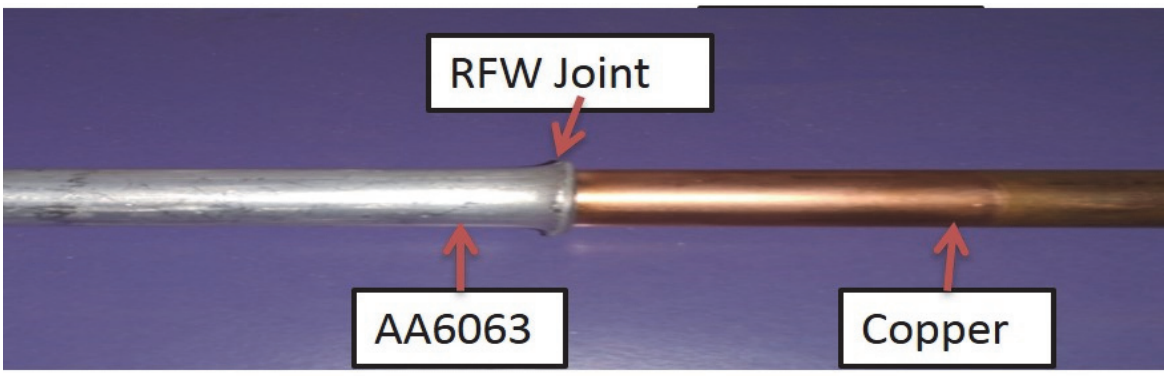

Figure 2(b): Specimens Prepared using AA6063 and Copper.

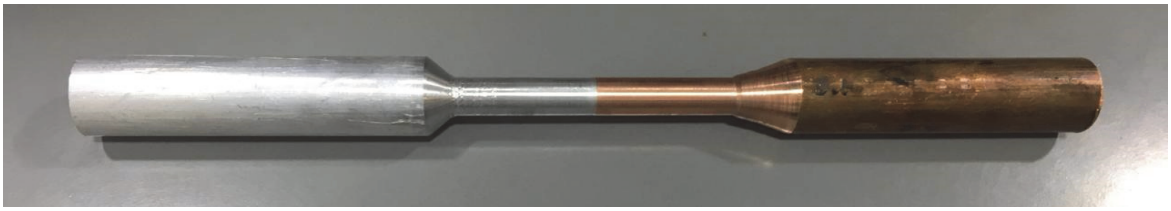

Figure 3: AA6063 and Copper welded specimen prepared for Tensile test.

The tensile testing experimentation has been carried out for the specimen of dimensions: 6mm gauge diameter, 50mm gauge length as prescribed by the ASTM standard in a computerized universal testing machine. The tensile tests have been carried out for AA6063-AISI4130 and AA6063-Cu welded specimens. The results of the experiment such as load and displacement are recorded and analyzed to evaluate the tensile strength. The three specimens were tested for each cases and average values have been listed in the Tab. 4. The standard deviations are ranging from 0.5 to 2.6.

RESULTS AND DISCUSSIONS

Optimization

The experimental values of the tensile strength of AA6063-AISI4130 and AA6063-Cu welded specimens were determined. The comparison of results of both the experimentations were listed in the Tab. 4. From comparison, it is seen that AA6063-AISI4130 dissimilar welded joints exhibits the better tensile strength than the AA6063-Cu welded joints.

Case	Friction Pressure MPa	Friction Time Sec	Upset Pressure MPa	Tensile Strength, MPa	
				AA6063-AISI4130	AA6063-Cu
1	48	2	38	223	154
2	48	4	68	266	196
3	48	6	97	248	183
4	71	2	68	271	200
5	71	4	97	301	222
6	71	6	38	285	201
7	97	2	97	247	182
8	97	4	38	259	181
9	97	6	68	268	198

Table 4: Tensile strength of AA6063-AISI4130 and AA6063-Cu for different welding conditions.

In comparison with the AA6063-Cu, the tensile strength of the AA6063-AISI4130 steel exhibits the highest tensile strength. The increased strength of AA6063-AISI4130 steel is due to the higher strength of the steel than the copper. For all cases of Taguchi's DOE, AA6063-AISI4130 steel provides the highest strength. The obtained results of the experimentations are the input functions for the Taguchi's analysis. Commercially available statistical tool is used to analyze the obtained result for AA6063-AISI4130 and AA6063-Cu dissimilar welding joints. The quality attributes were determined by transferring the results into the signal to noise(S/N) ratio. The influence of the process parameters like UP, FP and FT on the tensile strength of the AA6063-AISI4130 and AA6063-Cu dissimilar welding joints are analyzed using the signal to noise ratio.

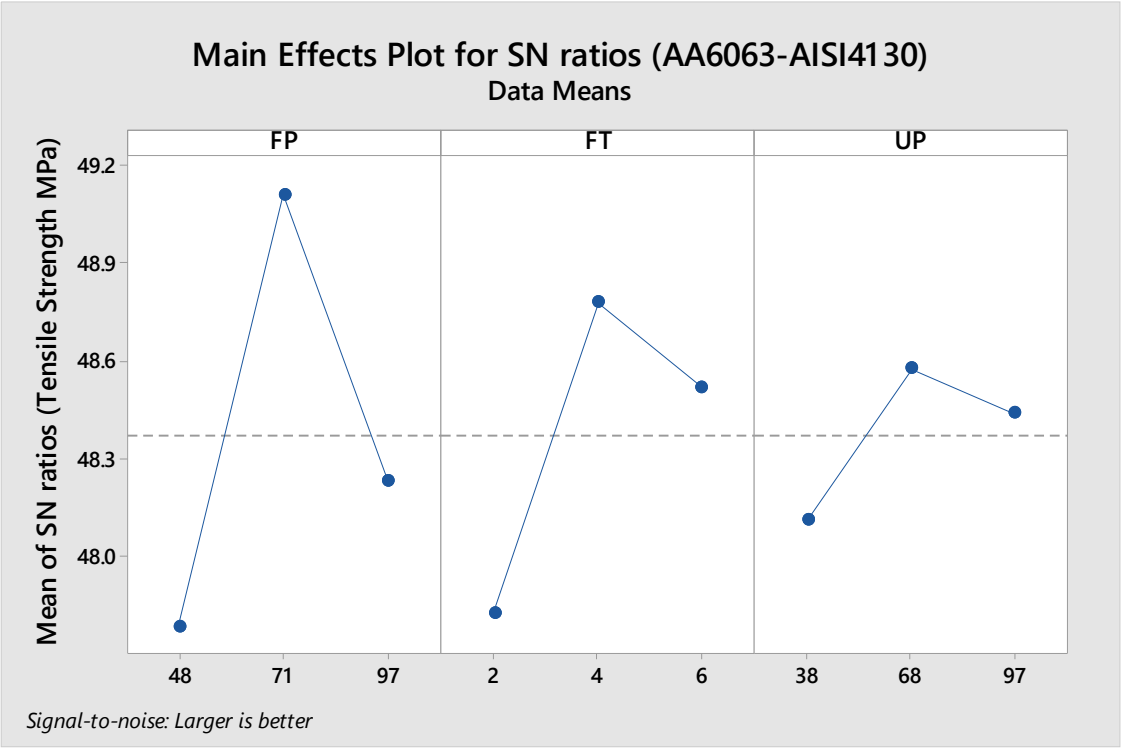

Figure 4(a): Main Effects plot for SN ratios – AA6063-AISI4130.

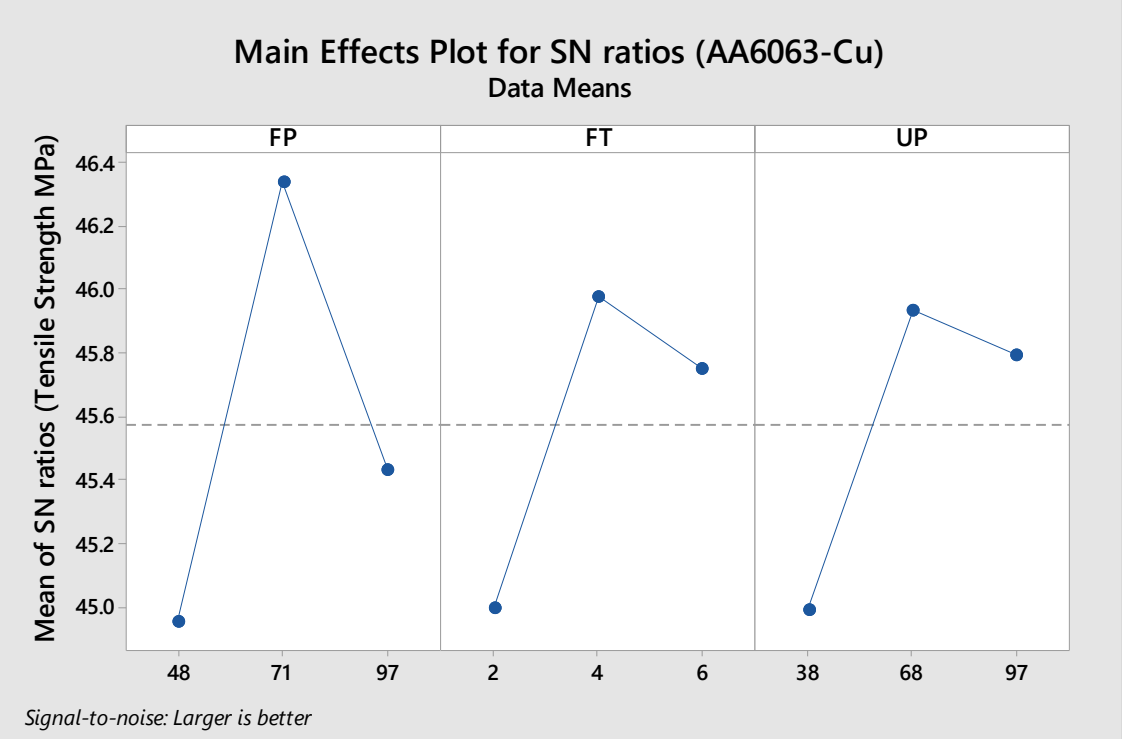

Figure 4(b): Main Effects plot for SN ratios – AA6063-Cu.

The factors FP, FT and UP are statistically major in the S/N ratio and are also observed that FP significantly influence results of the tensile strength followed by FT and UP. Fig. 4(a) and 4(b) displays the influence of the factors FP, FT and UP on the tensile strength of the said welded joints.

From Fig 4(a) and 4(b) it is seen that as the increment in the process parameters such as FT, FP and UP causes increment in the tensile strength initially for the both AA6063-AISI4130 and AA6063-Cu welded joints. Further increment in FP, FT and UP the decrement in the tensile strength has been observed. It is obvious that increment in the pressure deceases the strength of the welded joints.

ANalysis Of VAriance (ANOVA)

The experimental results, which inputted into the Taguchi's DOE, were analyzed using ANOVA. ANOVA gives the confidence level of each parameter and its percentage contribution on the tensile strength of the welded joints. The confidence level considered here is 95%, thus the significant level is 0.05. The contribution of each parameter on the strength is given in Tab. 5.

Source	Degrees of Freedom	Sequential Sum of Squares	Adjusted Mean Squares	F-Value	P-Value	% contribution
Friction Pressure	2	2517.56	1258.78	35.85	0.027	61.1
Friction Time	2	1272.22	636.11	18.12	0.052	30.9
Upset Pressure	2	262.89	131.44	3.74	0.211	6.3
Error	2	70.22	35.11	-	-	1.7
Total	8	4122.89	-	-	-	-

Table 5(a): ANOVA for tensile strength of AA6063-AISI4130.

From the Tab. 5(a) and 5(b) it has been seen that the FP has the significant effect about 61.1% and 50.3%on the tensile strength of AA6063-AISI4130 and AA6063-Cu respectively. Thus, the FP is the significant factor in the tensile strength of the AA6063-AISI4130 and AA6063-Cu joints followed by the FT about 30.9% and 25% whereas the UP have least influence (6.3% and 23.2%) on the tensile strength. The pooled error is only 1.7% and 1.5%. As a result of the investigation, it is advised that FP, followed by the FT and UP, has the major impact on the tensile strength of the mentioned dissimilar welds.

Source	Degrees of Freedom	Sequential Sum of Squares	Adjusted Mean Squares	F-Value	P-Value	% contribution
Friction Pressure	2	1402.57	701.28	32.86	0.03	50.3
Friction Time	2	697.71	348.85	16.34	0.058	25.0
Upset Pressure	2	648.09	324.05	15.18	0.062	23.2
Error	2	42.69	21.34	-	-	1.5
Total	8	2791.05	-	-	-	-

Table 5(b): ANOVA for tensile strength of AA6063-Cu.

Microstructure

Fig. 4(a) displays the optical microstructure of the AA6063-AISI4130 joint at the R/2 location. On the AA6063 side of the joint, there were primarily two zones: base material (BM) zone and heat-affected zone (HAZ). Between BM and HAZ, the dynamic recrystallized zone (DRZ) and thermal mechanically affected zone (TMAZ) can be found. The thermal-mechanical connection effect caused the interface temperature to rise quickly during friction welding, which encouraged the recovery and dynamic recrystallization of the aluminum alloy close to the interface. The microstructure evolved from fine, equiaxed grains to streamline shapes, leading to the formation of the dynamic recrystallized zone. In a transition zone (TMAZ), where most grains were bent, and most partial grains underwent dynamic recrystallization. Streamlines also underwent considerable plastic deformation, changing from their original straight to curved shape. Because the interface temperature, which was lower than that of fusion welding but still reached the dynamic recrystallization temperature, grains in the HAZ were smaller than those of the BM in Fig. 4(a). The joint also primarily had two zones on the AISI4130 side: the BM and HAZ. Because of broken of partial original grains, by increased UP at higher temperature along the interface, the grains in the HAZ on the AISI4130 side were finer.

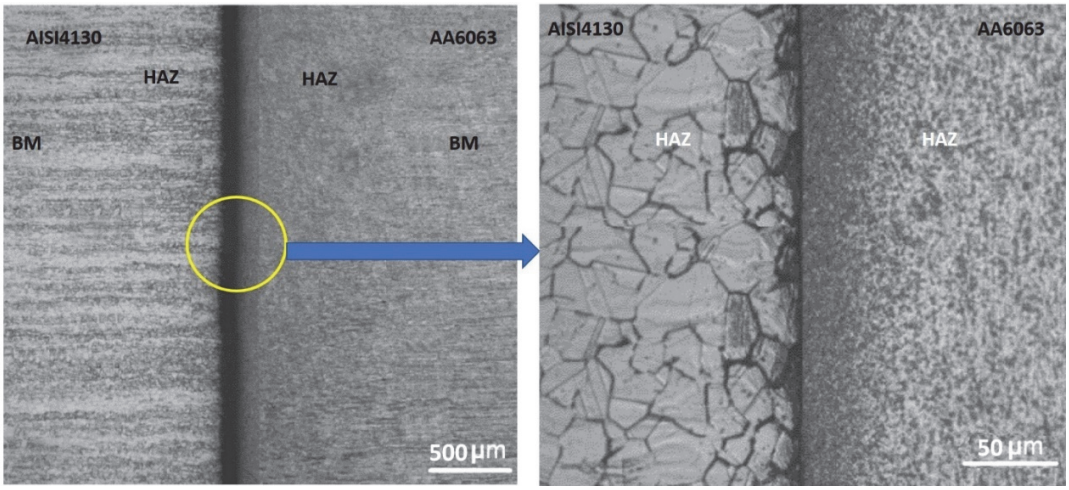

Figure 4(a) Optical microstructure at joint interface, BM, HAZ of AA6063-AISI4130

As shown in Fig. 4, the obvious reaction layer between AA6063 and AISI4130 developed with an average thickness of 2.5µm as a result of the shared distribution of alloying materials under the influence of thermo-mechanical coupling. The interface between reaction layer and AISI4130 was smooth, whereas the interface between reaction layer and AA6063 was rough as shown in Fig. 4(a), indicating that the reaction layer advance towards the side of AA6063. The microstructure of the reaction layer in the R/2 site under various welding circumstances is shown in Fig. 4(b). The thickness of the interfacial intermetallic compounds (IMC) initially declined with an upset pressure of 97 MPa, but it subsequently began to stabilize (approaching 2.50µm) as friction pressure increased.

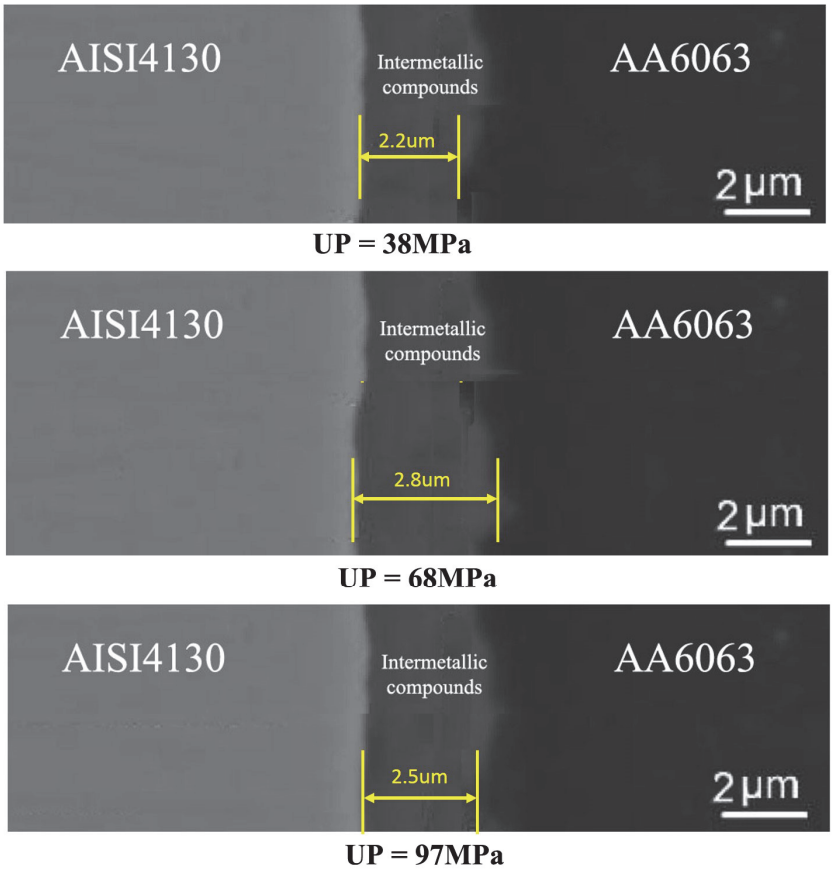

Figure 4(b) Interfacial microstructure of the joint for different UP of AA6063-AISI4130.

It was evident from the examination of the interfacial microstructure that excessive interfacial IMC thickness significantly reduced the UTS of AA6063-AISI4130 joint. In order to thoroughly extrude the oxidized metal and dangerous contaminants in the interface, which was advantageous to metallurgical reaction, it was profitable to increase upset pressure. The UTS of joints was improved by increasing upset pressure up to 97MPa with friction pressure of 71 MPa and friction time of 4 sec. According to the analysis above, the ideal parameters were FP=71MPa, FT=4sec, and UP=97MPa, with a maximum UTS of 301 MPa for the AA6063-AISI4130 joint.

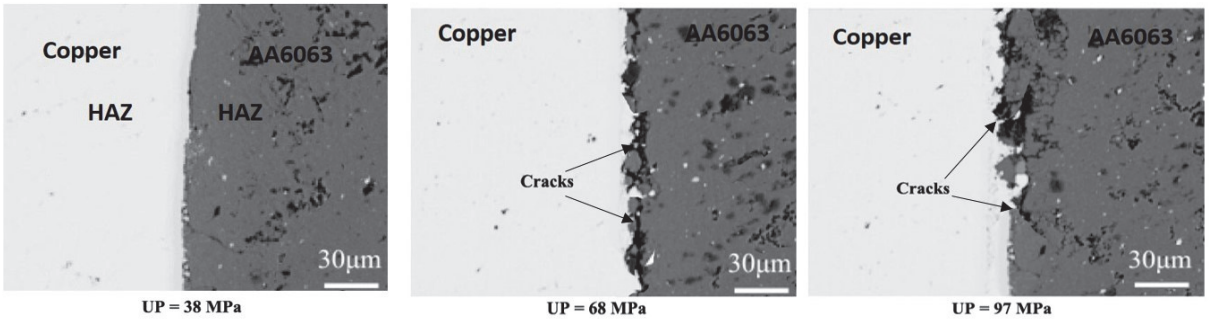

Figure 5(a): Optical microstructure at joint interface, BM, HAZ of AA6063-Copper

After UP of 68MPa, backscattered pictures at the interface show a decline in AA6063-Copper joint quality (Fig. 5(a)). At the interface center, a flaw in incomplete joining may be detected. Cracks developed in aluminum close to the interface at the R/2 and edge positions. Microcracks may be seen on the side of AA6063 in the backscattered picture at the edge position (Fig. 5(a)). From the Fig. 5(a), it can be observed that the propagation of irregular microcracks along the grain boundaries of AA6063 at edge position. The tensile strength of edge samples that underwent UP of 97MPa drastically decreased because of the presence of microcracks.

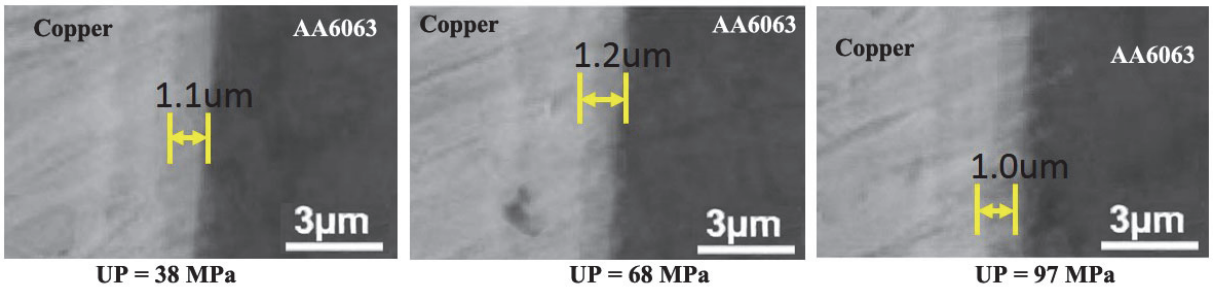

Figure 5(b) Interfacial microstructure of the AA6063-Copper joint for different UP

The interface of the two layers of the AA6063-Copper joint for different UP is given in Fig. 5(b). The dark IMC layer near the AA6063 appears to be Al_2Cu, and the other layer's composition is similar to Al_4Cu_9. Al_2Cu and Al_4Cu_9 layers can't be separated from one another because IMC layers are relatively flat and parallel in the centre. The thickness of IMC layers grows as the distance from the centre rises, and some minor IMC particles disperse in the AA6063 at the R/2 position. After UP of 38MPa, the IMC layer thickness slightly increases. The UTS of AA6063-Copper joint was improved by increasing upset pressure up to 97MPa with FP of 71 MPa and FT of 4 sec which gets the maximum UTS of 222 MPa.

Confirmation Experiment

The final step in design process is the confirmation experiment. The experimental outcomes attained must validate using the statistical analysis. The statistical analysis was determined using the regression equation carried out using MINITAB tool. The regression model gives the relation between the variable and the response, by fitting the linear equation to the existing data. The regression Eqns. 1 and 2 respectively obtained from the analysis of AA6063-AISI4130 and AA6063-Cu welded joints.

$$\text{Tensile strength of AA6063-AISI4130} = 211.8 + 0.285\ FP + 5.00\ FT + 0.165\ UP \quad (1)$$

Tensile strength of AA6063-Cu = 141.5 + 0.210 FP + 3.77 FT + 0.287 UP (2)

Case	AA6063-AISI4130 Tensile Strength, MPa			AA6063-Cu Tensile Strength, MPa		
	Experimental	Statistical	% error	Experimental	Statistical	% error
1	223	243	8.1	154	170	9.3
2	266	258	3.1	196	187	4.8
3	248	273	9.0	183	203	9.8
4	271	253	6.7	200	183	8.4
5	301	268	11.1	222	199	10.3
6	285	268	6.0	201	190	5.8
7	247	263	5.9	182	195	6.6
8	259	263	1.4	181	186	2.5
9	268	278	3.5	198	202	2.2

Table 6: Comparison of experimental and statistical results

According to the results of the ANOVA, FP is the most important factor that affects tensile strength, followed by FT, and UP is the least important component. The regression Eqns. 1 and 2 shows that an increase in the FP, FT, and UP results in an increase in the tensile strength which can be also seen in Fig 4. Tab. 6 compares the results of the experiment with the statistical conclusions drawn from the regression model. The experimental and statistical tensile strength values were observed to vary by an error percentage ranging from 1.4 to 11.1 percent for welded joints made of AA6063-AISI4130, whereas it varies from 2.2 to 10.3 percent for AA6063-Cu.

As a result, except for case 5, the tensile strength estimated by the experimental and regression models agree with one another, with an error rate of less than 10 percent. Hence the validation of experimental and statistical results, agree with each other and are within the permissible error [20].

CONCLUSIONS

The experimental work on RFW of AA6063-AISI4130 and AA6063-Cu dissimilar metal welded joints led to the following conclusions.

- The RFW of the dissimilar joints such as AA6063-AISI4130 and AA6063-Cu was successfully performed using different parameters. The maximum tensile strength obtained for the AA6063-AISI4130 is 26% higher than AA6063-Cu welded joints. This is a result of the use of AISI4130, which is stronger than copper and aluminum.
- The Taguchi's and ANOVA analysis reveals that the FP influences more on the tensile strength of mentioned welded joints followed by the FT and UP.
- The SEM micrographs reveals the formation of intermetallic compounds on the side of AA6063. The formation of microcracks is on the side of AA6063 which propagates along the grain boundaries at R/2 location. Thus, the failure occurs at the AA6063.
- The confirmation experiment through the statistical analysis agrees with the experimental results. Thus, the experimental results were validated.

FUNDING

This research received no specific grant from any funding agency in the public, commercial, or not-for-profit sectors.

CONFLICT OF INTEREST

The authors declare that they have no conflict of interest.

REFERENCES

[1] Patil, H. S., Patel, D. C. (2022). Al2O3 and TiO2 flux enabling activated tungsten inert gas welding of 304 austenitic stainless steel plates, Frattura ed Integrità Strutturale, 61, pp. 59-68. DOI: 10.3221/IGF-ESIS.61.04.

[2] El-Oualid, B., Chikh, S., Abdi, S., Miroud, D. (2017) Thermal analysis during a rotational friction welding. Appl Therm Eng 110, pp. 1543–1553. DOI: 10.1016/j.applthermaleng.2016.09.067.

[3] Emel, T., Gould, J.E., Lippold, J.C. (2010) Dissimilar friction welding of 6061-T6 aluminium and AISI 1018 steel: properties and microstructural characterisation. Mater Des 31, pp.2305–2311. DOI: 10.1016/j.matdes.2009.12.010

[4] Anthony, R.M., Colegrove, P.A., Buhr, C., Flipo, B.C.D., Vairis, A. (2018) A literature review of Ti-6AL-4V linear friction welding. Prog Mater Sci 92, pp. 225–257. DOI: 10.1016/j.pmatsci.2017.10.003

[5] Baffari, D., Buffa, G., Campanella, D., Fratini, L., Micari, F. (2014) Friction based solid state welding techniques for transportation industry applications. Procedia CIRP 18, pp. 162–167. DOI: 10.1016/j.procir.2014.06.125

[6] Kessler, M., Suenger, S., Haubold, M., Zaeh, M.F. (2016) Modelling of upset and torsional moment during inertia friction welding. JMaterProcess Technol 227, pp. 34–40. DOI: 10.1016/j.jmatprotec.2015.07.024

[7] Bounini, T., Bouchouicha, B., Ghazi, A. (2018). Simulation of the behavior of Aluminium Alloys welded in FSW (Case of AA5083, AA6082), Frattura ed Integrità Strutturale, 46, pp. 1-13. DOI: 10.3221/IGF-ESIS.46.01.

[8] Patil, C., Patil, H., Patil, H. (2016). Experimental investigation of hardness of FSW and TIG joints of Aluminium alloys of AA7075 and AA6061, Fattura ed Integrità Strutturale, 37, pp. 325-332; DOI: 10.3221/IGF-ESIS.37.43

[9] Hong, M., Qin, G., Geng, P., Fei, L., Banglong, F., Meng, X. (2015). Microstructure characterisation and properties of carbon steel to stainless dissimilar metal joint made by friction welding. Mater Des 86, pp. 587–597. DOI: 10.1016/j.matdes.2015.07.068

[10] Szávai, Sz., Bezi, Z., Ohms, C. (2016). Numerical simulation of dissimilar metal welding and its verification for determination of residual stresses, Frattura ed Integrità Strutturale, 36, pp. 36-45; DOI: 10.3221/IGF-ESIS.36.04.

[11] Nada, R., Arsic, D., Lazic, V., Nikolic, R.R., Hadzima, B. (2016). Microstructure in the joint friction plane in friction welding of dissimilar steels. Procedia Eng 149, pp. 414–420. DOI: 10.1016/j.proeng.2016.06.686.

[12] Ochi, H., Ogawa, K., Yamamoto, Y., Suga, Y. (1998) Friction welding of aluminium alloy and Steel. Int J Offshore Polar Eng 8(2), ISOPE-98-08-2-140.

[13] Ambroziak, A., Korzeniowski, M., Kustron, P., Winnicki, M., Sokolowski, P. and Jarapinska, E. (2014). Friction Welding Of Aluminium And Aluminium Alloys With Steel", Adv Mater Sci Eng, 2014. DOI: 10.1155/2014/981653

[14] Kimura, M., Suzuki, K., Kusaka, M., Kaizu, K. (2017). Effect of friction welding condition on joining phenomena and mechanical properties of friction welded joint between 6063 aluminium alloy and AISI 304 stainless steel. J Manuf Process 26, pp. 178–187. DOI: 10.1016/j.jmapro.2017.02.008

[15] Fukumoto, S., Inoue, T., Mizuno, S., Okita, K., Tomita, T., Yamamoto, A. (2010). Friction welding of TiNi alloy to stainless steel using Ni interlayer. Sci Technol Weld Join 15(2), pp. 124–130. DOI: 10.1179/136217109X12577814486692

[16] Suresh, D., Meshram, G., Madhusudhan, R. (2015). Friction welding of AA60612 to AISI 4340 using silver interlayer". Defence Technology 11, pp. 292–298. DOI: 10.1016/j.dt.2015.05.007

[17] Adrian, L., Mogami, H., Matsuda, T., Sano, T., Yoshida, R., Hori, H., Hirose, A. (2018) Hardening and softening effects in Aluminium alloys during high-frequency linear friction welding. J Mater Process Tech 255, pp. 547–558. DOI: 10.1016/j.jmatprotec.2018.01.002

[18] Ajith, P.M., Barik, B.K., Sathiya, P., Aravindan, S. (2015) Multi objective optimisation of friction welding of UNS S32205 duplex stainless steel. Defense Technology 11, pp. 157–165. DOI: 10.1016/j.dt.2015.03.001

[19] Saleemsab, D., Yasmin, B., Bharath, K. N., Rajesh, A. M., Kaleemulla, M. K. (2020). Optimization of process parameters of fracture toughness using simulation technique considering aluminum-graphite composites, Transactions of the Indian Institute of Metals, Springer, 73(12) (2020), pp. 3095 – 3103. DOI: 10.1007/s12666-020-02113-5.

[20] Guddhur, H., Naganna, C., Doddamani, S. (2021). Taguchi's method of optimization of fracture toughness parameters of Al-SiCp composite using compact tension specimens. An International Journal of Optimization and Control: Theories &Amp; Applications (IJOCTA), 11(2), pp. 152–157. DOI: 10.11121/ijocta.01.2021.00990.
[21] Vishalkumar, D., Ambad, A. K., Saleemsab, D. (2020). Optimization of process parameters for fracture toughness of Al6061-graphite composites, Structural Integrity and Life, 20(1), pp 51–55.
[22] Hareesha, G., Chikkanna, N., Saleemsab, D., Anilkumar, S. K. (2021). Effect of addition of SiC particles on the microstructure and hardness of Al-SiC composite, Metallurgical and Materials Engineering, 27(1), pp. 49-56. DOI: 10.30544/590.
[23] Chaib, M., Slimane, A., Slimane, S., Ziadi, A., M., Bouchouicha, B., (2021). Optimization of Ultimate Tensile Strength with DOE Approach for Application FSW Process in the Aluminum alloys AA6061-T651 & AA7075 -T651, Frattura ed Integrità Strutturale, 57, pp. 169-181. DOI: 10.3221/IGF-ESIS.57.14
[24] Hong, M., Qin, G., Geng, P., Li, F., Meng, X., Banglong, F. (2016) Effect of post-weld heat treatment on friction welded joint of carbon steel to stainless steel. J Mater Process Technol 227, pp. 24–33. DOI: 10.1016/j.jmatprotec.2015.08.004
[25] Patil, H. S., Soman, S. N. (2013). Effect of weld parameter on mechanical and metallurgical properties of dissimilar joints AA6082–AA6061 in T6 condition produced by FSW, Frattura ed Integrità Strutturale, 24, pp. 151-160; DOI: 10.3221/IGF-ESIS.24.16.
[26] Mekri, H., Bouchouicha, B., Miloudi, A., Christophe, H., Imad, A. (2018). Influence of the coupling between the mechanical characteristics and the welding conditions by the FSSW process: case of the bi-material aluminum-steel, Frattura ed Integrità Strutturale, 46, pp. 62-72. DOI: 10.3221/IGF-ESIS.46.07
[27] Besel, Y., Besel, M., Alfaro Mercado, U., Kakiuchi, T., Uematsu, Y. (2016). Influence of joint line remnant on crack paths under static and fatigue loadings in friction stir welded Al-Mg-Sc alloy, Frattura ed Integrità Strutturale, 35 , pp. 295-305; DOI: 10.3221/IGF-ESIS.35.34
[28] Morales, C., Merlin, M., Fortini, A., Garagnani, G.L., Miranda, A. (2022). Impact behavior of dissimilar AA2024-T351/7075-T651 FSWed butt-joints: effects of Al2O3-SiC particles addition, Frattura ed Integrità Strutturale, 60, pp. 505-515. DOI: 10.3221/IGF-ESIS.60.34
[29] Senthil Murugan, S., Noorul Haq, A., Sathiya, P. (2020). Effect of welding parameters on the microstructure and mechanical properties of the friction-welded dissimilar joints of AA6063 alloy and faying surface-tapered AISI304L alloy, Welding in the World, 64, pp. 483–499. DOI: 10.1007/s40194-020-00846-x.
[30] Souza Neto, F., Neves, D., Silva, O. M. M., Lima, M. S. F., Abdalla, A.J. (2015). An Analysis of the Mechanical Behavior of AISI 4130 Steel after TIG and Laser welding process, Procedia Engineering, 114, pp. 181 – 188. DOI: 10.1016/j.proeng.2015.08.057.
[31] https://matweb.com, Copper, Cu; Data Sheet.